ChemComm

COMMUNICATION

View Article Online
View Journal | View Issue

Cite this: *Chem. Commun.*, 2023, 59, 418

Received 16th November 2022,
Accepted 6th December 2022

DOI: 10.1039/d2cc06188k

rsc.li/chemcomm

Highly efficient light-induced self-assembly of gold nanoparticles promoted by photoexcitation-induced aggregatable ligands†

Xiaoyan Xu,[a] Man Zhang,[a] Zhongyu Li,[a] Danfeng Ye,[a] Lizhen Gou,[c] Qi Zou *[bc] and Liangliang Zhu *[a]

There are numerous ways to achieve light-induced self-assembly of gold nanoparticles, but most of them are through chemical reaction and slow. Ligands that can perform photoexcitation-induced aggregation were synthesized and modified onto gold nanoparticles. The leading functionalized nanoparticles exhibit highly efficient light-induced self-assembly properties and show high-contrast color fading in tens of seconds.

Gold nanoparticles (Au NPs), enabling unique electronic and optical properties, size controllability, surface chemistry modifiability, and facile synthesis, are promising in a wide variety of applications, such as electrochemical sensors,[1] catalysis,[2] and disease treatment.[3] Light-induced self-assembly (LISA) of Au NPs has attracted considerable attention, because light is a kind of precise, contactless, and less invasive external stimulus, and compared to other external stimuli, it can be applied and removed instantaneously. A number of publications have reported varying methods to endow Au NPs with the ability of LISA, such as photodimerization,[4–6] photothermally triggered interaction,[7] light-triggered host–guest interaction,[8,9] photoacid generator-mediated H bonds,[10,11] participation of light-reduced silver,[12] light-triggered covalent formation,[13] and photoisomerization.[14–16] Although there have been a lot of scientific achievements in the control of LISA, the applied photoresponsive molecular types remain limited, and the formation of large-size assembly of Au NPs always requires tens of minutes or even hours.

In the present study, lipoic acid ester and lipoamide-modified persulfurated benzene compounds (denoted as **1** and **2**, see chemical structures in Fig. 1a, as well as synthetic details in the ESI†) were designed and synthesized as photoresponsive ligands. Persulfurated benzenes are a kind of asterisk-shaped molecule with twisted structures, which show photosensitivity through the rotation of the flexible C–S–C bonds under illumination.[17–19] Due to this intriguing structure, persulfurated benzenes exhibit significant conformational differences of molecular geometry between the ground and the excited states.[17–19] The molecular conformational change is reflected in the change of C_1–C_2–S–C_3 and C_2–S–C_3–C_4 bond-rotation (based on our previous geometric study,[17,18,20] the torsion of C_1–C_2–S–C_3 varied from approximately 118° to 80° along with that of C_2–S–C_3–C_4 from 44° to 15°). Compared to the ground state conformation, the excited state conformation facilitates molecular aggregation,[21,22] *viz.* photoexcitation-induced molecular aggregation. In other words, the aggregation process of photoexcited persulfurated benzenes is straightforward, which is quite different from those photochemical cases followed by self-assembly. Inspired by the specific photoexcited-induced aggregation properties of persulfurated benzenes, we prepared Au NPs surface modified with **1** and **2**, respectively, and comprehensively studied their LISA performances. Benefitting from the direct aggregation effect of persulfurated benzene ligands, the composite Au NPs were able to form large-size aggregates with around 1 μm diameter under *in situ* photoirradiation in 3 min (Fig. 1b) with high-contrast color tuning.

It is noteworthy that the photoexcitation-induced aggregation of persulfurated benzene ligands is self-recoverable, and this was confirmed by light switching in dynamic light scattering (DLS) experiments. As shown in Fig. 2a and b, the photo-induced assembly–disassembly cycle could be carried out at least 5 times. Before UV irradiation, ligand **1** was relatively dispersed (~2 nm), and after a short period (10 s) of 365 nm irradiation, the molecules formed aggregates (18–33 nm), proving the high aggregation efficiency of ligand **1**. On the contrary,

[a] *State Key Laboratory of Molecular Engineering of Polymers, Department of Macromolecular Science, Fudan University, Shanghai 200438, China. E-mail: zhuliangliang@fudan.edu.cn*
[b] *Key Laboratory for Advanced Materials and Feringa Nobel Prize Scientist Joint Research Center, Frontiers Science Center for Materiobiology and Dynamic Chemistry, School of Chemistry and Molecular Engineering, East China University of Science and Technology, Shanghai 200237, China. E-mail: zouqi@ecust.edu.cn*
[c] *Shanghai Key Laboratory of Materials Protection and Advanced Materials in Electric Power, Shanghai University of Electric Power, Shanghai, 200090, China*
† Electronic supplementary information (ESI) available. See DOI: https://doi.org/10.1039/d2cc06188k

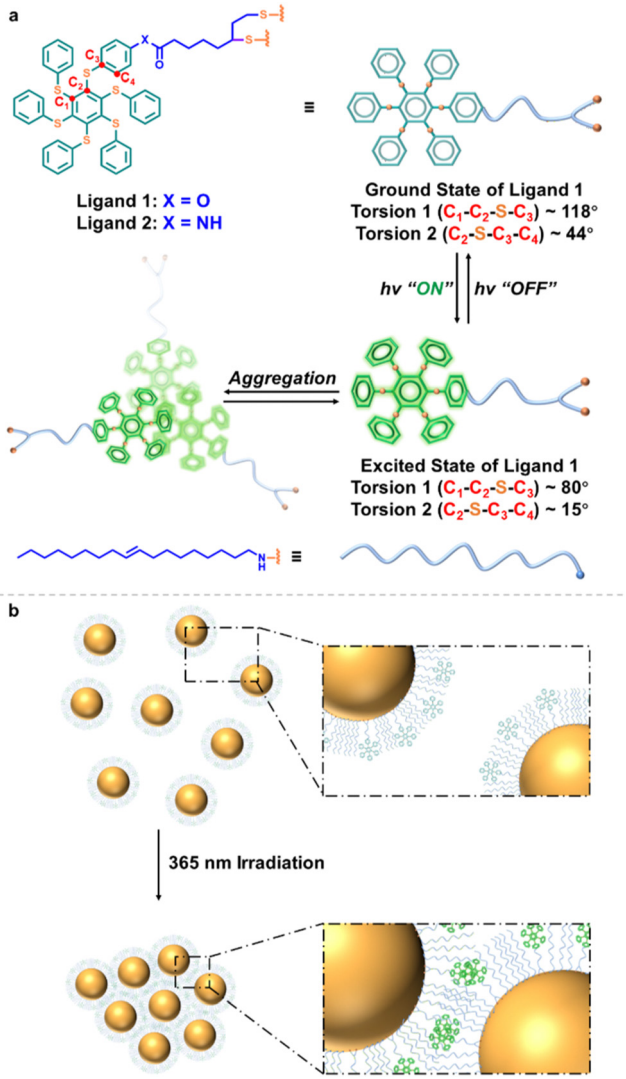

Fig. 1 (a) Chemical structure of oleylamine, **1**, and **2**, as well as the mechanism of photoexcitation-induced conformational change and aggregation of **1** and **2**. The oleamine plays the role of solubilizer, reductant, and stabilizer in the reduction of chloroauric acid to gold nanoparticles. (b) Light-induced self-aggregation of **1-Au NPs**.

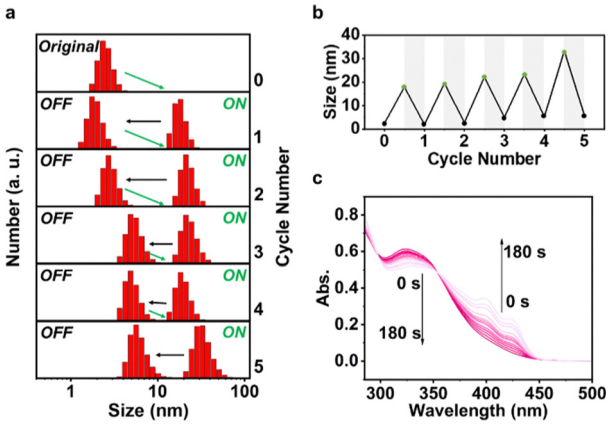

Fig. 2 (a) Five assembly–disassembly cycles of **1** in toluene solution (1×10^{-3} M) as followed by DLS. Ligand **1** assembled under 365 nm irradiation for 10 s, and disassembled in the dark for 15 min. (b) Average particle size change calculated by (a). (c) Continuous monitoring of UV-vis spectra of ligand **1**.

the self-recovery is slow, and a pronounced fatigue effect was observed.[23] After being left in the dark for 15 min, the particle size was restored to around 2 nm in the first cycle but increased slightly in the subsequent cycles. Unsurprisingly, ligand **2** also exhibited similar switchable photo-induced assembly-disassembly behavior (Fig. S15, ESI†). However, its original size was almost twice as large as that of ligand **1** (~4 nm), and a more obvious fatigue effect can be visually observed in Fig. S15b (ESI†). This can be largely attributed to the kinetically trapped effect of the intermolecular H bonds between amide groups.[20,24]

Absorption changes of **1** and **2** were also investigated (Fig. 2c and Fig. S16, ESI†). Two new absorption bands centred at 397 nm and 420 nm appeared upon irradiation, signifying that aggregated chromophore species formed.[25] Along with the extension of the irradiation time, new-emerged bands increased gradually, while the original one at 324 nm decreased, corresponding to the increase and decrease of the number of dispersions and aggregates, respectively. This behaviour is consistent with the DLS result, further confirming the photoexcitation-induced aggregation of **1** and **2**.

Next, we synthesized oleamine-stabilized Au NPs as control ones with uniform size of around 9 nm (Fig. S17a and c, ESI†) in toluene solution. Upon irradiation with 365 nm UV light for 3 min, such a dispersion of Au NPs was hardly affected, according to the TEM images and absorption spectra (Fig. S17, ESI†). Then, persulfurated benzene-modified Au NPs (named **1-Au NPs** and **2-Au NPs**) were prepared by simply mixing ligands and Au NPs. And to find out the optimal grafting density of ligands, we prepared a series of **1-Au NPs** by stirring solutions with a specific concentration (26.9 nM) of Au NPs and gradient concentration of ligand **1** ranging from 0.001 M to 0.020 M for 1 h (named **1-Au NPs-0.001**, ..., **1-Au NPs-0.020**, Table S1, ESI†). As Au NPs exhibit localized surface plasmon resonance (LSPR) in connection with particle size and shape, environment, assembly, and composition,[26] the assembly of Au NPs under UV irradiation can be studied by means of absorption spectra.

1-Au NPs were irradiated with 365 nm UV light for 3 min, and the absorption spectrum was continuously monitored during this process (Fig. 3a and Fig. S18, ESI†). Before UV irradiation, there was a narrow characteristic absorption band assigned to LSPR at 529 nm. The red shift relative to oleamine-stabilized Au NPs (524 nm, Fig. S17d, ESI†) was caused by a slight assembly of ligands **1** and in turn the aggregation of **1-Au NPs** to a small extent. Upon UV irradiation, the LSPR absorbance intensity at 529 nm reduced and became broader, while the absorption in the long wavelength range belonging to aggregates of Au NPs enhanced gradually, signifying the immediate formation of the large aggregates of Au NPs and the lessening of the original particles. Meanwhile, in the

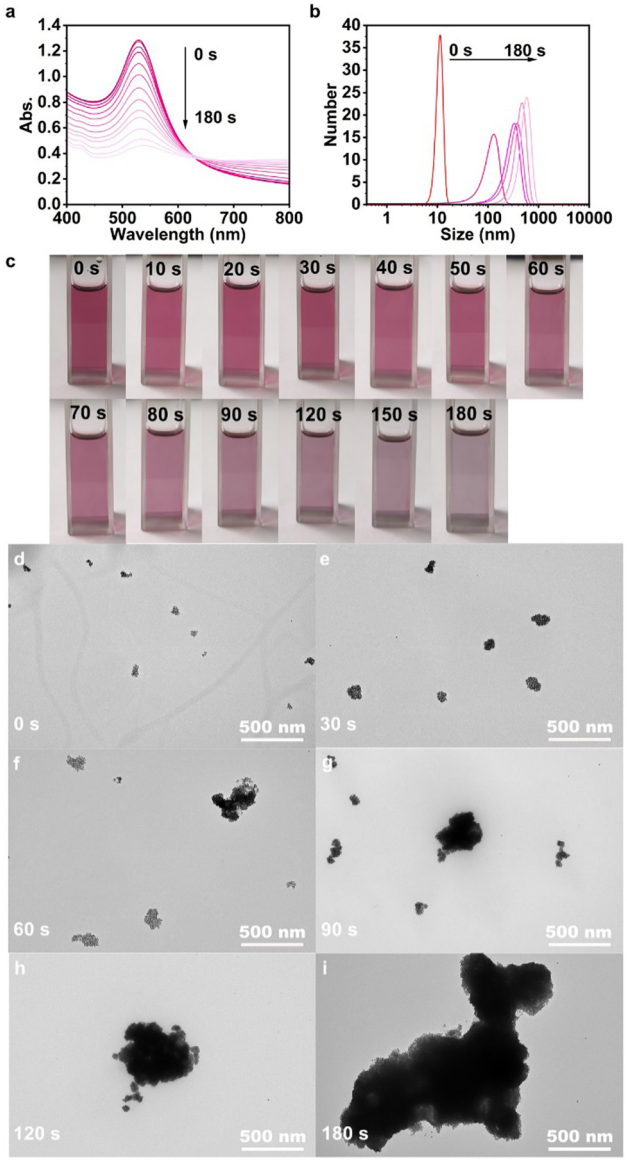

Fig. 3 Continuous monitoring of (a) UV-vis spectra, (b) DLS signal, (c) photographs, and (d–f) TEM images of **1-Au NPs-0.008** under 365 nm light irradiation for 3 min.

absorption spectra of samples **1-Au NPs-0.005**, **1-Au NPs-0.008**, **1-Au NPs-0.010**, **1-Au NPs-0.015**, and **1-Au NPs-0.020**, the absorption bands of the aggregates of ligands at 420 nm were observed after UV irradiation for about 90 s. The appearance of these peaks demonstrated that ligand **1** aggregated on the surface of **1-Au NPs** by photoexcitation. Due to the low grafting density of **1**, aggregation signals of **1** in both **1-Au NPs-0.001** and **1-Au NPs-0.003** could not be monitored.

As expected, a critical amount of **1** per Au NP played an important role in achieving high-efficiency LISA of **1-Au NPs**. When the amount of **1** is low, the self-assembly efficiency is naturally low. However, in the case of too high an amount of **1**, the persulfurated benzenes were first consumed to self-assemble with the adjacent persulfurated benzenes on their host Au NP, leading to low LISA efficiency as well. The normalization of the LSPR absorbance intensity change as a function of irradiation time was integrated into Fig. S18h (ESI†), suggesting that **1-Au NPs-0.008** was the most efficient sample of LISA. And the degree of color change shown in the insets of Fig. S18a–g (ESI†) also confirmed this. Therefore, **1-Au NPs-0.008** was chosen for more detailed research, and the grafting density of **1** on **1-Au NPs-0.008** (1.16 nm^{-2}) was calculated from the result of thermal gravimetric analysis (TGA, Fig. S19, ESI†).

Dynamic light scattering (DLS) was selected to investigate the variation of the aggregate size of **1-Au NPs-0.008** with UV irradiation time. As shown in Fig. 3b, the original particles were as small as 10 nm and uniformly dispersed, and aggregated at an extremely fast speed under irradiation. The dispersed particles self-assembled into large aggregates over 100 nm in 30 s, and super aggregates up to 1 μm in 3 min. The continuous change of sample color was also monitored with photographs (Fig. 3c). At first, the sample appeared rosy red, then became more and more transparent, and slightly purple, corresponding to the weakening of the LSPR peak and the enhancement of the long-wavelength absorption. Besides, it was perceived that a thin layer of black precipitate gradually accumulated at the bottom of the cuvette, which also indicates the rapid formation of super aggregates. Fig. 3d–i illustrates the time-related TEM images of **1-Au NPs-0.008** under UV irradiation. Apparently, well-dispersed Au NPs were observed initially that transformed into tremendous aggregates step by step after UV irradiation within 3 min. Undoubtedly, both the macro appearances and microstructures fully confirmed the LISA of **1-Au NPs-0.008**. Furthermore, Fourier-transform infrared (FTIR) of **1-Au NPs-0.008** before and after UV irradiation for 3 min (Fig. S20, ESI†) was carried out in order to exclude the possibility that photochemical reaction led to the aggregation of Au NPs. The spectra remained consistent with no peak shift, which demonstrated that the LISA of **1-Au NPs** was a physical process (namely, photoexcitation-induced assembly) instead of a photochemical behavior. Besides, the absence of signal shifts in the ^{1}H NMR of ligands **1** and **2** under continuous irradiation (Fig. S21, ESI†) also confirmed the high photochemical stability of the compounds.

As a control, a rough study was also made on **2-Au NPs-0.008** (Fig. S22, ESI†). On the one hand, **2-Au NPs-0.008** had similar LISA behavior and efficiency as **1-Au NPs-0.008**. On the other hand, its initial size was larger than that of **1-Au NPs-0.008** owing to the H bonds between ligands **2** as mentioned above, and hence the LSPR peak of **2-Au NPs-0.008** (534 nm) was bathochromically shifted relative to **1-Au NPs-0.008** (529 nm), and the color of **2-Au NPs-0.008** was more purplish. Obviously, although the H bonds between lateral groups had some effect on the self-assembly of Au NPs before irradiation, the photoexcitation-induced aggregation of persulfurated benzenes was the main driving force leading to the LISA of Au NPs.

Recently, the remote control of the luminescence and discoloration behavior of materials has been widely used in information technology.[27–30] In view of the highly efficient LISA feature, persulfurated benzene-modified Au NPs show potential

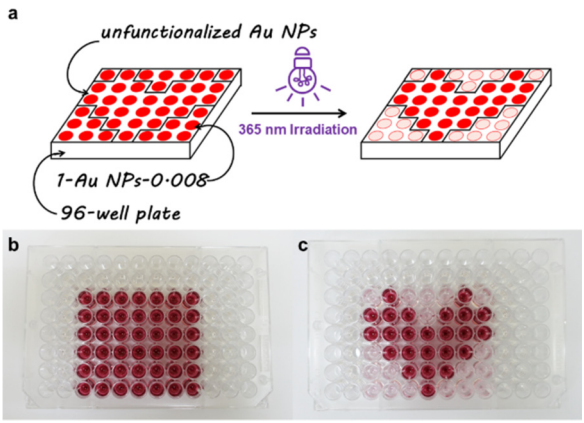

Fig. 4 (a) Schematic representation of a set-up to create a heart-shaped image using light. Photographs of the set-up (b) before and (c) after 365 nm irradiation for tens of seconds for macroscopic information encryption.

in macroscopic information encryption. The specific method was to ''draw'' information to be conveyed with unfunctionalized Au NPs on a 96 well plate, and then fill the remaining wells with persulfurated benzene-modified Au NPs as ''background''. In the original state, the pattern was red, displaying no information, but after UV irradiation, the ''background'' became colorless, thereby displaying the encrypted information. In this work, we ''drew'' a heart pattern with unfunctionalized Au NPs and used **1-Au NPs-0.008** to fill the ''background''. Next, we irradiated the 96 well plate with a 365 nm UV lamp for tens of seconds, and the ''heart'' emerged accompanied by the color fading of the ''background'' (Fig. 4).

In summary, we synthesized persulfurated benzene ligands and constructed a highly efficient LISA of Au NPs through a fast photoresponsive supramolecular system. The photoexcitation-induced aggregation properties of **1** and **2** have been studied comprehensively. Different from traditional photoresponsive self-assembly ligands, their self-assembly under UV irradiation is straightforward due to the direct molecular aggregation driven by molecular conformation transition from the ground state to the excited state. Thus, persulfurated benzene-modified Au NPs exhibited high LISA efficiency with high-contrast color fading characteristics. The effect of grafting density and hydrogen bonds between the side groups on the LISA of **1-Au NPs** was also investigated. Owing to the rapid discoloration, we can use the functionalized and unfunctionalized Au NPs to draw patterns and backgrounds to simply realize macroscopic information encryption. This work on incorporating a new type of photo-responsive molecule with nanosystems can bring inspiration in promoting the advances of controlled visualized applications.

This work was supported by NSFC/China (22275038, 21975046, and 22175064), and partially by the Natural Science Foundation of Shanghai (20ZR1421700).

Conflicts of interest

There are no conflicts to declare.

Notes and references

1 M. Chelly, S. Chelly, R. Zribi, H. Bouaziz-Ketata, R. Gdoura, N. Lavanya, G. Veerapandi, C. Sekar and G. Neri, *Nanomaterials*, 2021, **11**, 739.
2 L. Zhu, H. Yan, C. Y. Ang, K. T. Nguyen, M. Li and Y. Zhao, *Chem. – Eur. J.*, 2012, **18**, 13979–13983.
3 C. Li, K. Feng, N. Xie, W. Zhao, L. Ye, B. Chen, C.-H. Tung and L.-Z. Wu, *ACS Appl. Nano Mater.*, 2020, **3**, 5070–5078.
4 H. He, M. Feng, Q. Chen, X. Zhang and H. Zhan, *Angew. Chem., Int. Ed.*, 2016, **55**, 936–940.
5 Y. Chen, Z. Wang, Y. He, Y. J. Yoon, J. Jung, G. Zhang and Z. Lin, *Proc. Natl. Acad. Sci. U. S. A.*, 2018, **115**, E1391–E1400.
6 A. F. De Fazio, A. H. El-Sagheer, J. S. Kahn, I. Nandhakumar, M. R. Burton, T. Brown, O. L. Muskens, O. Gang and A. G. Kanaras, *ACS Nano*, 2019, **13**, 5771–5777.
7 D. Fava, M. A. Winnik and E. Kumacheva, *Chem. Commun.*, 2009, 2571–2573.
8 L. Stricker, E. C. Fritz, M. Peterlechner, N. L. Doltsinis and B. J. Ravoo, *J. Am. Chem. Soc.*, 2016, **138**, 4547–4554.
9 J. Wu, Y. Xu, D. Li, X. Ma and H. Tian, *Chem. Commun.*, 2017, **53**, 4577–4580.
10 P. K. Kundu, D. Samanta, R. Leizrowice, B. Margulis, H. Zhao, M. Borner, T. Udayabhaskararao, D. Manna and R. Klajn, *Nat. Chem.*, 2015, **7**, 646–652.
11 Y. Cheng, J. Dong and X. Li, *Langmuir*, 2018, **34**, 6117–6124.
12 S. J. Zhen, Z. Y. Zhang, N. Li, Z. D. Zhang, J. Wang, C. M. Li, L. Zhan, H. L. Zhuang and C. Z. Huang, *Nanotechnology*, 2013, **24**, 055601.
13 J. Lai, Y. Xu, X. Mu, X. Wu, C. Li, J. Zheng, C. Wu, J. Chen and Y. Zhao, *Chem. Commun.*, 2011, **47**, 3822–3824.
14 R. Klajn, P. J. Wesson, K. J. Bishop and B. A. Grzybowski, *Angew. Chem., Int. Ed.*, 2009, **48**, 7035–7039.
15 D. Huebner, C. Rossner and P. Vana, *Polymer*, 2016, **107**, 503–508.
16 Q. Wang, D. Li, J. Xiao, F. Guo and L. Qi, *Nano Res.*, 2019, **12**, 1563–1569.
17 X. Jia, C. Shao, X. Bai, Q. Zhou, B. Wu, L. Wang, B. Yue, H. Zhu and L. Zhu, *Proc. Natl. Acad. Sci. U. S. A.*, 2019, **116**, 4816–4821.
18 T. Weng, Q. Zou, M. Zhang, B. Wu, G. V. Baryshnikov, S. Shen, X. Chen, H. Agren, X. Jia and L. Zhu, *J. Phys. Chem. Lett.*, 2021, **12**, 6182–6189.
19 B. Yue, X. Feng, C. Wang, M. Zhang, H. Lin, X. Jia and L. Zhu, *ACS Nano*, 2022, **16**, 16201–16210.
20 J. Gu, B. Yue, G. V. Baryshnikov, Z. Li, M. Zhang, S. Shen, H. Agren and L. Zhu, *Research (Wash D C)*, 2021, 9862093.
21 Y. Gong, M. Zhang, X. Jia, B. Yue and L. Zhu, *Langmuir*, 2021, **37**, 14398–14406.
22 B. Yue, X. Jia, G. V. Baryshnikov, X. Jin, X. Feng, Y. Lu, M. Luo, M. Zhang, S. Shen, H. Agren and L. Zhu, *Angew. Chem., Int. Ed.*, 2022, **61**, e202209777.
23 R. Klajn, *Chem. Soc. Rev.*, 2014, **43**, 148–184.
24 S. Shen, G. Baryshnikov, B. Yue, B. Wu, X. Li, M. Zhang, H. Ågren and L. Zhu, *J. Mater. Chem. C*, 2021, **9**, 11707–11714.
25 Y. Li, G. V. Baryshnikov, C. Xu, H. Agren, L. Zhu, T. Yi, Y. Zhao and H. Wu, *Angew. Chem., Int. Ed.*, 2021, **60**, 23842–23848.
26 V. Amendola, R. Pilot, M. Frasconi, O. M. Maragò and M. A. Iatì, *J. Phys.: Condens. Matter*, 2017, **29**, 203002.
27 B. Li, Z. Li, K. You, A. Qin and B. Z. Tang, *Sci. China: Chem.*, 2022, **65**, 771–777.
28 W. C. Xu, C. Liu, S. Liang, D. Zhang, Y. Liu and S. Wu, *Adv. Mater.*, 2022, **34**, e2202150.
29 Q. Wang, Z. Qi, Q.-M. Wang, M. Chen, B. Lin and D.-H. Qu, *Adv. Funct. Mater.*, 2022, 2208865.
30 Q. Niu, P. Jin, Y. Huang, L. Fan, C. Zhang, C. Yang, C. Dong, W. Liang and S. Shuang, *Analyst*, 2022, **147**, 880–888.